Journal of Muscle Research and Cell Motility (2005) 26:259–273
DOI 10.1007/s10974-005-9043-4

Controlled intermittent shortening contractions of a muscle–tendon complex: muscle fibre damage and effects on force transmission from a single head of rat EDL

HUUB MAAS[1,2,†], T. MAARIT LEHTI[3,†], VENDLA TIIHONEN[4], JYRKI KOMULAINEN[3,4] and PETER A. HUIJING[1,5,*]
[1]*Instituut voor Fundamentele and Klinische Bewegingswetenschappen, Faculteit Bewegingswetenschappen, Vrije Universiteit, Van der Boechorststraat 9, 1081 BT, Amsterdam, The Netherlands;* [2]*School of Applied Physiology, Georgia Institute of Technology, 281 Ferst Drive, Atlanta, GA, 30332–0356, USA;* [3]*LIKES-Research Center for Sport and Health Sciences, FIN-40700, Jyväskylä, Finland;* [4]*Neuromuscular Research Center, Department of Biology of Physical Activity, University of Jyväskylä, FIN-40351, Jyväskylä, Finland;* [5]*Integrated Biomedical Engineering for Restoration of Human Function, Instituut voor Biomedische Technologie, Faculteit Constructieve Technische Wetenschappen, Universiteit Twente, NL-7500 AE, Enschede, The Netherlands*

Received 12 July 2005; accepted in revised form 12 October 2005

Abstract

This study was performed to examine effects of prolonged (3 h) intermittent shortening (amplitude 2 mm) contractions (muscles were excited maximally) of head III of rat extensor digitorum longus muscle (EDL III) on indices of muscle damage and on force transmission within the intact anterior crural compartment. Three hours after the EDL III exercise, muscle fibre damage, as assessed by immunohistochemical staining of structural proteins (i.e. dystrophin, desmin, titin, laminin-2), was found in EDL, tibialis anterior (TA) and extensor hallucis longus (EHL) muscles. The damaged muscle fibres were not uniformly distributed throughout the muscle cross-sections, but were located predominantly near the interface of TA and EDL muscles as well as near intra- and extramuscular neurovascular tracts. In addition, changes were observed in desmin, muscle ankyrin repeat protein 1, and muscle LIM protein gene expression: significantly ($P < 0.01$) higher (1.3, 45.5 and 2.3-fold, respectively) transcript levels compared to the contralateral muscles. Post-EDL III exercise, length-distal force characteristics of EDL III were altered significantly ($P < 0.05$): at high EDL III lengths, active forces decreased and the length range between active slack length and optimum length increased. For all EDL III lengths tested, proximal passive and active force of EDL decreased. The slope of the EDL III length-TA + EHL force curve decreased, which indicates a decrease of the degree of intermuscular interaction between EDL III and TA + EHL. It is concluded that prolonged intermittent shortening contractions of a single head of multi-tendoned EDL muscle results in structural damage to muscle fibres as well as altered force transmission within the compartment. A possible role of myofascial force transmission is discussed.

Introduction

The concept of myofascial force transmission is based on the phenomenon that, in addition to transmission between sarcomeres in series, force can be transmitted from sarcomeres within muscle fibres to the surrounding endomysium (Street and Ramsey, 1965; Street, 1983). Within muscle fibres adjacent parallel sarcomeres are linked to each other by desmin at the Z-line (Lazarides, 1980) and by skelemin at the M-line (Price, 1987; Price and Gomer, 1993). Complexes of structural proteins located between sarcomeres, subsarcolemmal cytoskeleton and extracellular matrix (e.g. dystroglycan protein complex reviewed in Berthier and Blaineau, 1997) connect muscle fibres to the intramuscular connective tissue network. Experimental evidence for myofascial force transmission (for reviews see Huijing, 1999; Monti *et al.*, 1999) indicates that these linkages are stiff enough to transmit force. Although not directly measured, several groups have agreed that the most likely mechanism for such force transmission is by shearing of these structures (Tidball, 1991; Trotter, 1993; Boriek *et al.*, 2001; Purslow, 2002; Kjaer, 2004).

Within sarcomeres, titin connects thick (myosin) filaments to the Z-line at both sides. Therefore, titin as well as titin-associated and Z-line proteins are in a good position to act as sensors for sarcomere strain.

* To whom correspondence should be addressed. Phone: +31-20-4448476; Fax: +31-20-4448529; E-mail: p_a_j_b_m_huijing@fbw.vu.nl)

† H. Maas and T.M. Lehti contributed equally to this work.

Potential examples of these kind of proteins are the titin-associated proteins, muscle ankyrin repeat protein 1 (MARP1) and muscle LIM protein (MLP) (reviewed in Knoll *et al*., 2003; Miller *et al*., 2004).

Under isometric conditions, it has been shown that myofascial pathways transmit force from a single muscle head of extensor digitorum longus muscle (EDL) to the bony skeleton. EDL is a multi-tendoned muscle that consists of four heads of which the muscle fibres share a common aponeurosis and tendon proximally, but have individual aponeuroses and tendons distally (for images see Balice-Gordon and Thompson, 1988; Maas *et al*., 2003). Experiments on fully dissected EDL indicated that force is transmitted between muscle heads via their connective tissue interface (i.e. intramuscular myofascial force transmission) (Huijing *et al*., 1998). For EDL muscle within an intact compartment, it has been reported that force is transmitted between a muscle head and (a) adjacent muscles, via connective tissue at the interface between the muscle bellies, (called intermuscular myofascial force transmission) and/or (b) surrounding non-muscular structures, via other extramuscular connective tissues (called extramuscular myofascial force transmission) (Maas *et al*., 2003). The results of a recent study indicated that *intra*muscular and *extra*muscular myofascial force transmission may also be present during shortening contractions of a single EDL head (Maas and Huijing, 2005).

During shortening of a single head of EDL, the position of that head relative to adjacent tissues is altered, which involves shearing of the interface between these structures. Finite element modelling has indicated that the highest shear strains and stresses maybe found in the muscle belly near the tendon that had changed length (Yucesoy *et al*., 2003). In this study, it is hypothesized that the frequent occurrence of such high strains and stresses may lead to local disturbances or altered mechanical properties of the structures providing the myofascial route of force transmission. Disruption of certain proteins linking sarcomeres and the endomysium may lead to the damage of muscle fibres.

The aim of the present study was to investigate effects of prolonged (3 h) intermittent shortening contractions of rat EDL III on (a) structural proteins of muscle fibres involved in muscular force transmission and on (b) force transmission between EDL III and adjacent tissues of the intact anterior crural compartment. Specific immunohistochemical stainings of structural proteins were used to estimate muscle fibre damage in the early phase (3 h post-exercise) and gene expression was measured to indicate changes of regulation of particular proteins. For histology, both a protein related to strain in muscle fibre direction (titin) and proteins related to myofascial pathways of force transmission (desmin, dystrophin, laminin−2) were selected. In addition to titin and desmin, MARP1 and MLP were selected for gene expression studies because of their fast response to exercise (Barash *et al*., 2004) and postulated role on stretch sensing (Miller *et al*., 2004).

Methods

Surgical and experimental procedures were in strict agreement with the guidelines and regulations concerning animal welfare and experimentation set forth by Dutch law, and approved by the Committee on Ethics of Animal Experimentation at the *Vrije* Universiteit, Amsterdam, The Netherlands. Immediately after the muscles were excised, the animals were killed using an overdose of pentobarbital and double-sided pneumothorax.

Surgical procedures

Male Wistar rats ($n = 11$, body mass = 311.2 g SD 20.2, ≈9 weeks old) were anaesthetized using intraperitoneally injected urethane (1.2 ml/100 g body mass 12.5% urethane solution, extra doses were given if necessary: maximally 1.5 ml), which is known to provide long periods of anaesthesia with minimal physiological changes (Field and Lang, 1988). To prevent hypothermia during surgery and data collection, the animals were placed on a heated water pad of approximately 37°C. Ambient temperature (22°C SD 0.5) and air humidity (80% SD 2) were kept constant. Dehydration of muscle and tendon tissue was prevented by regular irrigation with isotonic saline.

The anterior crural compartment of the left hind limb, which envelopes the tibialis anterior (TA), EDL and extensor hallucis longus (EHL) muscles was exposed. Connective tissues of the compartment at the muscle bellies of TA, EHL and EDL as well as the retinaculae at the ankle were left intact. In the foot, the distal tendon of head III of EDL muscle (further referred to as EDL III) as well as the distal tendons of TA and EHL muscles were dissected free from surrounding tissues. With the ankle joint at 90°, the distal tendons of TA and EHL muscles were tied together using polyester thread (further referred to as TA + EHL). The distal tendons of EDL III and TA + EHL were cut and Kevlar threads (diameter = 0.5 mm, tensile modulus = 58 GPa, 3.7% extension to breaking; Goodfellow) were tied to them. The foot was attached to a plastic plate with tie wraps. The femoral compartment was opened in order (a) to cut a small piece of the lateral epicondyle of the femur (i.e. the origin of EDL muscle) for attaching it to Kevlar thread, (b) to secure a metal clamp to the femur for later fixation in the experimental apparatus, and (c) to dissect the sciatic nerve.

The tibial nerve, the sural branch as well as all proximal branches of the sciatic nerve were cut. The sciatic nerve, with only the common peroneal nerve branch left intact, was dissected and cut as proximally

as possible. Branches of the common peroneal nerve innervate EDL, EHL and TA muscles as well as the muscles in the peroneal compartment.

Mounting the animal in the experimental apparatus

A more detailed description of the experimental set-up can be found in a previous paper (Maas *et al*., 2003). The femur was secured at a knee angle of 100° and with the plastic footplate the ankle angle was set to 90° (Figure 1). Using the Kevlar threads, the proximal tendon of EDL muscle as well as the distal tendons of TA + EHL were connected to force transducers (maximal output error <0.1%, compliance of 0.0048 mm/N; Hottinger Baldwin) mounted on single axis micropositioners, and the distal tendon of EDL III was connected to a strain gauge force transducer (compliance 0.014 mm N^{-1}) mounted on a multipurpose muscle ergometer (Woittiez *et al*., 1987). Kevlar threads for TA + EHL and EDL III force measurements were guided via a pulley to the force transducers (Figure 1).

The sciatic nerve, with only the common peroneal nerve branch left intact, was placed on a pair of silver electrodes. The nerve was prevented from dehydrating, by covering it with paper tissue saturated with isotonic saline covered by a thin piece of latex. In all experimental conditions, the sciatic nerve was stimulated supramaximally using electrodes connected to a constant current source (3 mA, pulse width 100 μs).

Experimental protocol

For all experimental conditions, the length of the TA + EHL complex was kept constant (corresponding to an ankle joint angle of 90°). Also the position of the proximal tendon of EDL muscle was kept constant (corresponding to a knee joint at 100°). In addition, the distal tendons of EDL head II, IV, and V were left attached to their insertions on the foot. Therefore, their muscle–tendon complex lengths were also kept constant. Exclusively, the muscle–tendon complex length of EDL III was manipulated experimentally. Before acquiring data, the EDL muscle was preconditioned by isometric contractions at several high lengths of EDL III until isometric forces at low and high EDL III length were reproducible (i.e. equal values in repeated measurements) (Maas *et al*., 2003).

Assessment of isometric length–force characteristics of EDL III and the simultaneous measurements of isometric forces exerted at the proximal EDL tendon and the distal TA + EHL tendons was performed prior to (pre) and after (post) 3 h of intermittent shortening contractions of EDL III. After the cessation of exercise, the muscles were allowed to recover until (a) EDL and TA + EHL forces were not further increasing, but remained at a constant level (approximately after 12 min, tested in one animal), and (b) the force trace resembled that of an isometric contraction of the muscle in the unfatigued state (i.e. approximately after 20 min).

Isometric length–distal force characteristics of the EDL head III

Isometric force was measured at various muscle–tendon complex lengths of EDL III. EDL III was lengthening distally with 1 mm increments starting at active slack length (i.e. the lowest length at which active force approaches zero) until approximately 2 mm beyond optimum length (l_o). Before each contraction, passive EDL III was brought to the desired length by moving the ergometer. Two twitches were evoked, followed by a tetanic contraction of the muscles after 500 ms (pulse train 400 ms, frequency 100 Hz). Passive isometric muscle force was measured just prior to tetanic contraction and total isometric muscle force was measured during the tetanic plateau of the muscles (i.e. 275 ms after evoking tetanic stimulation). Timing of stimulation of the nerve and A/D conversion (12-bit A/D converter, sampling frequency 1000 Hz, resolution of force 0.01 N) were controlled by a special-purpose microcomputer. After each contraction, EDL III was allowed to recover near active slack length for at least 2 min.

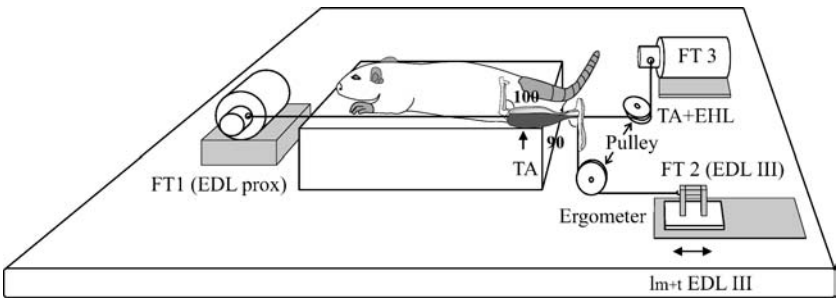

Fig. 1. Schematic representation of the experimental set-up. FT1 indicates the force transducer connected to the proximal tendon of EDL muscle. FT2 indicates the force transducer mounted on a multipurpose muscle ergometer connected to the distal tendon of EDL III. FT3 indicates the force transducer connected to the tied distal tendons of TA and EHL muscles. Kevlar thread was used to connect the muscles to force transducers. A low friction pulley guided the Kevlar thread from TA + EHL to FT3 that, for reasons of space, was placed perpendicular to the other force transducers. The proximal tendon of EDL muscle was connected directly to the force transducer, which was positioned in the line of pull. The distal tendon of EDL III was connected to the force transducer via a low friction pulley. Various muscle–tendon complex lengths of EDL III were obtained by repositioning FT2, as indicated by the double arrow.

Three hour exercise: intermittent shortening contractions of EDL III (n=8)

Passive EDL III was lengthened distally from l_o−2 mm to l_o in 0.5 s. Subsequently, stimulation of the common peroneal nerve and shortening of EDL III were started simultaneously. EDL III was allowed to shorten over a limited length range (i.e. from l_o to l_o−2 mm in 0.5 s). The duration of one stretch-shortening cycle was 1 s (i.e. frequency = 1 Hz). Pilot experiments revealed that the duration of relaxation of EDL III after a tetanic contraction was maximally 0.15 s. To prevent EDL III from being exposed to any lengthening contractions, nerve stimulation was turned off after 0.35 s, i.e. well before the onset of muscle–tendon complex lengthening. In Figure 2, it is clearly shown that the muscle was fully relaxed before lengthening was applied. Note that active shortening of EDL III follows a sinusoidal trajectory in time, i.e. length and shortening velocity change in time according to sinusoidal curves (maximal velocity = 6.28 mm/s). Such intermittent shortening contractions of EDL III were continued for an extended period of 3 h. Note that the other heads of EDL muscle as well as TA and EHL muscles were excited also intermittently for 3 h, but these muscles did not change muscle–tendon complex length during the experiment.

Post-exercise rest

Muscle damage induced by exercise as such may take some time to develop. Therefore, the muscles were allowed to rest for three hours after the cessation of EDL III exercise. This period was deemed long enough to detect at least very early signs of developing damage. The duration of this period was limited by the total time available for surgery and experimentation on each day.

Muscle sampling

Whole EDL muscle and the TA + EHL complex of both hind limbs were excised after 3 h of post-exercise rest, according to the following procedures: The distal ends of the tendons of head II, IV and V of EDL muscle were cut and tied to the distal tendon of EDL

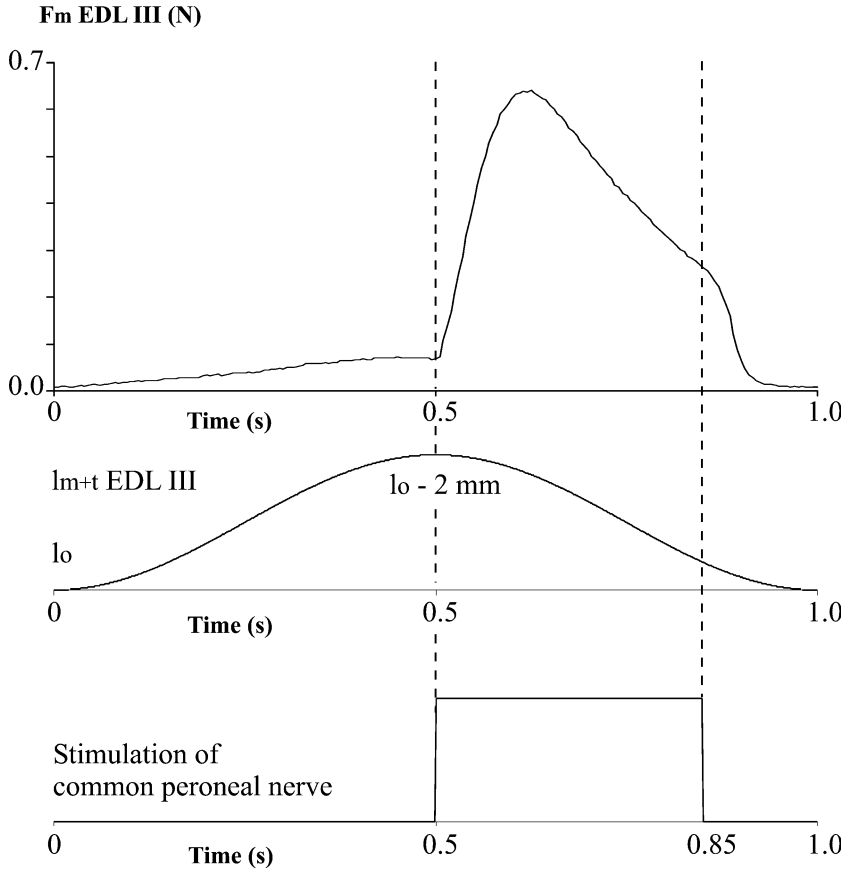

Fig. 2. A typical example of EDL III force during one cycle of intermittent shortening exercise of EDL III. Muscle–tendon complex length of EDL III and stimulation of the common peroneal nerve are shown. Passive EDL III was lengthened distally from l_o−2 mm to l_o in 0.5 s. Accordingly, force exerted at the distal tendon of EDL III increased. Subsequently, stimulation of the common peroneal nerve (exciting EDL, TA, EHL muscles as well as muscles in the peroneal compartment) and shortening of EDL III were started simultaneously. EDL III was allowed to shorten over a limited length range (i.e. from l_o to l_o−2 mm in 0.5 s). Note that active shortening of EDL III follows a sinusoidal trajectory in time. After building up of force, EDL III force decreased progressively. To prevent the muscle from being exposed to lengthening contractions, nerve stimulation was turned off after 0.35 s. Prior to the start of a subsequent stretch-shortening cycle, EDL III was fully relaxed.

III at a length corresponding to an ankle joint angle of 90°. The retinaculae at the ankle were severed. The anterior crural compartment was opened by full lateral fasciotomy and the muscles were marked (1% Brilliant Cresyl Blue solution, w/v, Sigma, St. Louis, USA) for anatomical orientation at the most medial and the most lateral location of the dorsal side of EDL muscle (i.e. the side adjacent to the anterior intermuscular septum, see open arrow heads, Figure 4). EDL muscle and the TA + EHL complex were separated, weighed, and frozen in isopentane cooled to freezing point (−160°C). All samples were stored at −70°C until further analyses.

Immunohistochemistry

In a cryostat at −20°C, a block (thickness 3–5 mm) of the mid-belly region of the muscle samples was cut with a razor blade perpendicular to the line of pull of the muscle and mounted with O.C.T. embedding compound (Tissue Tek7, Miles Laboratories, Elkhart, IN). A cross-section of EDL muscle at mid-belly region will likely include muscle fibres of all four heads (Maas *et al*., 2003). After trimming the block face, serial transverse sections (10 μm) were cut. Unstained EDL sections were photographed to visualize the Brilliant Cresyl Blue marks and thus define the anatomical orientation. Sections were stained for hematoxylin and eosin to verify overall histopathological changes. Additional serial sections were stained for titin (1:2000, monoclonal anti-titin clone T11, Sigma), desmin (1:100, Zymed Laboratories, San Francisco, CA), dystrophin (1:500, dys2, Novocastra Laboratories, Newcastle, U.K.), and laminin−2 (rabbit polyclonal anti-laminin−2, 1:500). The transverse sections were incubated overnight with dilutions of the primary antibody in a humidified chamber at +4°C. After washing with Tris-buffered saline (TBS, pH 7.5) the bound primary antibodies were visualized by avidin-biotin peroxidase kit (Vectastain PK−4002 for desmin, dystrophin, titin, and PK−4001 for laminin−2, Vector Laboratories, Burlingame, CA) using diaminobenzidine (Abbott Laboratories, Abbott Park, IL) as the chromogen. The sections were contrasted with hematoxylin staining.

Images were captured by a video camera (Sanyo High Resolution CCD, Sanyo, Osaka, Japan) mounted on a microscope (Olympus BX−50, Olympus, Tokyo, Japan). These images were used to evaluate the extent and location of muscle damage. Only fibres with complete absence of staining for dystrophin, desmin, as well as titin were counted and their locations within the muscle cross-section were determined.

Analyses of specific gene expression

For total RNA isolation, a piece of frozen EDL (~55 mg) was cut from the proximal muscle and homogenized with FastPrep homogenizer and FastPrep Green tubes (Qbiogen, Carlsbad, CA) in 1 ml Trizol reagent (Invitrogen, Carlsbad, CA). Isolation was performed according to the manufacturer's instructions. Concentration of total RNA was measured photometrically at 260 nm and the purity of RNA was assessed based on 260 nm/280 nm absorption ratio of ~2.0. Total RNA (5 μg) was reverse transcribed using High-Capacity cDNA Archive Kit (Applied Biosystems, Foster City, CA) according to manufacturer's instructions.

Primers for real-time PCR were designed and/or analyzed by Oligo Explorer and Analyzer software (http://www.uku.fi/~kuulasma/OligoSoftware/index.htm). Primers from the literature were used for GAPDH (housekeeping gene) (Spofford and Chilian, 2003), MARP1 (Barash *et al*., 2004), and MLP (Barash *et al*. 2004). Although the primers for MLP (NM_057144) and MARP1 (NM_013220) were designed for the mouse, considering the similarity between rat and mouse sequence, it seems appropriate to use them in the present study on rat transcripts. For rat desmin and titin primer design sequences Des, NM_022531 and Ttn, AF525411 were used (Table 1). Because Ttn sequences codes for cardiac isoform, binding of primers to the conservative sequence was verified by alignment with human Ttn mRNA sequence prominent in skeletal muscle (NM_133378). A sample of cDNA (5 ng RNA equivalent) was analyzed with QuantiTect SYBR Green PCR-kit (Qiagen GmbH, Hilden, Germany) and ABI Prism 7700 (Applied Biosystems). All samples were run in triplicate. The amplification was performed at the following temperatures: 95°C for 15 min, followed by 40 cycles at 94°C for 15 s, followed by 30 s at annealing temperature, 30 s at 72°C, and finally 15 s at the detection temperature. Annealing and detection temperatures are shown in Table 1. Specific mRNAs in the sample were quantified according to the standard curve measured along with the samples from dilution series of muscle cDNA. To compensate for variations in mRNA quantity and reverse transcription efficiency, the results were normalized to GAPDH. GAPDH transcript level measured from cDNA (5 ng RNA equivalent) of exercised and control EDL muscles were similar ($P = 0.94$). The specificity of the amplified target sequence was confirmed on observing a single reaction product of the right size on an agarose gel and a single peak on the DNA melting temperature curve determined at the end of the reaction.

Treatment of data and statistics

The individual muscle–tendon complex length (l_{m+t}) – passive muscle force (F_{mp}) data were fitted with an exponential curve, using a least-squares criterion. For each muscle–tendon complex length studied, active muscle force (F_{ma}) was assessed by subtracting fitted F_{mp} from total muscle force (F_m). These, $l_{m+t} - F_{ma}$ data were fitted by a polynomial. The order of the polynomial most adequately describing the relationship was selected, using a stepwise polynomial regression procedure.

Table 1. Primers for quantitative real-time PCR

	Primers	Prod /bp	Ann /°C	Det /°C
GAPDH*	For: 5′-GCCAAAAGGGTCATCATCTC-3′ Rev: 5′-GGCCATCCACAGTCTTCT-3′	225	50	80
MLP†	For: 5′-GAAGTTAATGGAGGCTGGAGC-3′ Rev: 5′-TCTCTGTCCTTGGCATTGAG-3′	213	54	76
MARP1†	For: 5′-GAAGTTAATGGAGGCTGGAGC-3′ Rev: 5′-TTCTCTGTCCTTGGCATTGAG-3′	244	54	80.5
Des (NM_022531)	For: 5′-CTTCAGGAACAGCAGGTC-3′ Rev: 5′-ATCTCGCAGGTGTAGGAC-3′	245	52	83
TTN (AF525411), (NM_133378)	For: 5́-AGAGGTGAAGCAAGAAGCA-3́ Rev: 5́-GATAGGCATGGTTGGGAT-3́	114	50	80.5

Forward (For) and reverse (Rev) primers, PCR product size (Prod), annealing temperature (Ann) and detection temperature (Det) used in the study.
*Spofford and Chilian (2003), †Barash *et al.* (2004).

Fitted curves were used to calculate mean data and standard deviations (SD) as well as to determine optimal force and optimum muscle–tendon complex length. Muscle–tendon complex length was expressed as the deviation from active slack length (Δl_{m+t}). Although forces exerted at the distal tendons of EDL III and the TA + EHL complex are in opposite direction to forces exerted at the proximal tendon of EDL, all forces are presented as positive values.

To test for effects of EDL III exercise on length–force characteristics of EDL III as well as on proximal EDL and TA + EHL forces, two-way ANOVAs for repeated measures (factors: l_{m+t} EDL III and EDL III contraction protocol) were performed. If significant main effects were found, Bonferroni *post hoc* tests were executed to further locate significant differences. A paired samples *t*-test was used to test (a) for effects of EDL III exercise on the length of EDL III at which proximal EDL force was maximal, (b) for differences in mass between the muscles of the contralateral and the experimental legs, and (c) for differences in gene expression of EDL muscles of the contralateral and experimental legs. *P* values <0.05 were considered statistically significant.

Results

Muscle wet weight

For EDL as well as TA + EHL, the mean wet muscle mass was significantly higher (9.1 %, SD 6.6 and 8.8 %, SD 3.6, respectively) for the muscles of the experimental leg compared to the muscles of the contralateral leg (Table 2).

Histology

Three hours after the cessation of exercise some swollen muscle fibres were observed in EDL, as well as in TA + EHL. These fibres are characterized by a more rounded appearance and larger cross-sectional area compared to surrounding fibres. Such features are considered as typical early indices of muscle fibre damage (Friden *et al.*, 1991; Komulainen *et al.*, 1998).

In addition, immunohistochemistry was used to characterize changes in cytoskeletal proteins (titin, desmin) as well as a subsarcolemmal protein (dystrophin) and an extracellular matrix protein (laminin−2). Discontinuous (i.e. fragmented) dystrophin staining was found beneath the sarcolemma for a number of swollen fibres. None of the cross-sections of the contralateral EDL, TA or EHL muscles showed any indices of early phase muscle damage as indicated by light microscopy of muscle cross-sections (Table 2). Some heavily damaged fibres in EDL, TA and EHL muscles were found to be dystrophin, desmin, and titin negative (Figure 3a–c, Table 2) and, in most cases, have also less dense or discontinuous laminin−2 staining (Figure 3d). Thus, damage was located in structures supporting the contractile system as well as intracellular and extracellular force transmitting structures.

The damaged muscle fibres were not distributed uniformly throughout the muscle cross-sections

Table 2. Muscle wet mass and the number of damaged muscle fibres (i.e. dystrophin, desmin as well as titin negative) of EDL muscle and the TA + EHL complex of the experimental leg and the contralateral leg

	Muscle wet mass (mg)		Damaged muscle fibres (#)	
	EDL	TA + EHL	EDL	TA + EHL
Experimental	184.8 (24.0)*	746.3 (30.3)**	14.8 (18.2)	4.8 (3.7)
Contralateral	169.5 (20.3)	686.7 (36.1)	0	0

Values are means (SD); $n = 8$, except for muscle wet mass of TA + EHL $n = 7$.
$^{**}P < 0.01$, $^{*}P < 0.05$ compared to the muscles of the contralateral leg.

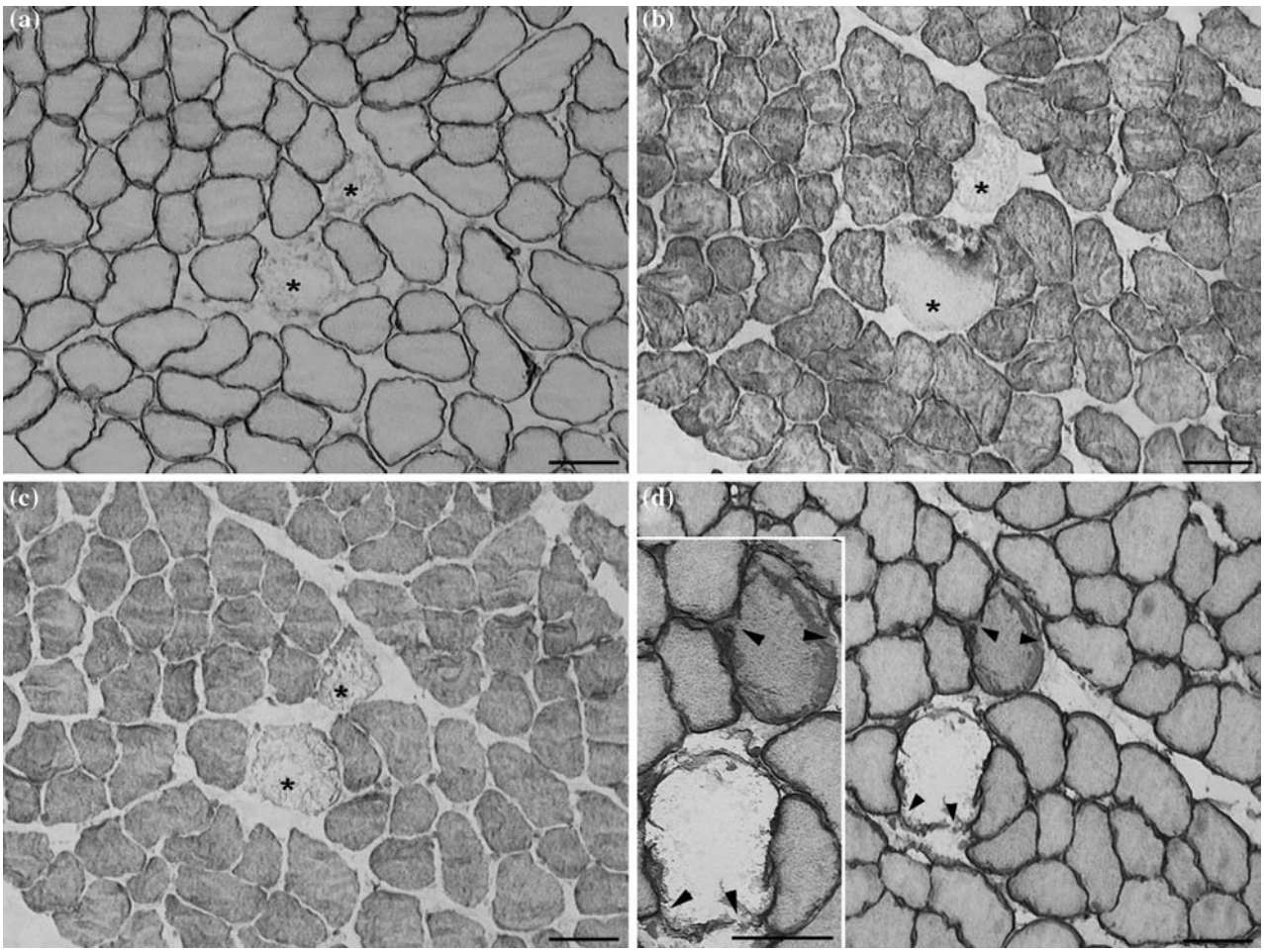

Fig. 3. An example of immunohistochemical observations 3 h post-EDL III exercise. Serial sections stained for dystrophin (a), desmin (b), titin (c), and laminin−2 (d) are shown. Some fibres of EDL, TA and EHL muscles were found to be dystrophin, desmin as well as titin negative (*) and with discontinuous laminin−2 (arrow head) staining. Discontinuous laminin−2 staining is more clearly seen with higher magnification (inset). Bar = 100 μm.

(Figure 4). Substantial individual variation between experiments was found regarding exact location of the lesions. However, damaged fibres within EDL muscle were located predominantly near the medial and ventral aspect of the EDL interface with TA muscle. Note that this is near the intramuscular and extramuscular neurovascular tracts. Damaged TA muscle fibres were located predominantly laterally near the interface with EDL muscle. Damaged EHL muscle fibres were medially near the location of the extramuscular neurovascular tract at a more distal muscle level.

Specific gene expression

For four muscle-specific proteins, mRNA levels were analyzed by real-time PCR: (1) Desmin (Des) and (2) titin (Ttn) that also showed changes in the histological analysis, and two titin associated proteins, (3) MLP, and (4) MARP1. The transcript levels for Des, MARP1 and MLP of the exercised EDL muscle were significantly higher than the contralateral EDL: 1.3 ($P < 0.01$), 45.5 ($P < 0.001$), and 2.3-fold ($P < 0.01$), respectively. In contrast, transcript level of Ttn showed no significant change (Figure 5).

Acute mechanical effects of changes of EDL III muscle–tendon complex length on isometric forces

To assess force transmission between EDL III and adjacent tissues via myofascial pathways of the intact anterior crural compartment, effects of EDL III length changes on forces exerted at the proximal tendon of EDL, as well as the distal tendons of TA + EHL were measured. To check if the above described post exercise early changes in structural proteins of muscle fibres also lead to altered mechanical properties of the pathways of which they are a part, these measurements were performed pre- and post-exercise. For data obtained prior to the prolonged intermittent shortening exercise of EDL III, ANOVA showed significant effects of EDL III muscle–tendon complex length on isometric forces exerted at the distal EDL III tendon, the proximal EDL tendon force and the distal TA + EHL tendons.

Distal EDL III force (Figure 6a)

Passive force was zero at low EDL III lengths and increased exponentially after lengthening EDL III distally ($F_{mp,\ peak} = 0.10$ N, SD 0.07). Optimum length

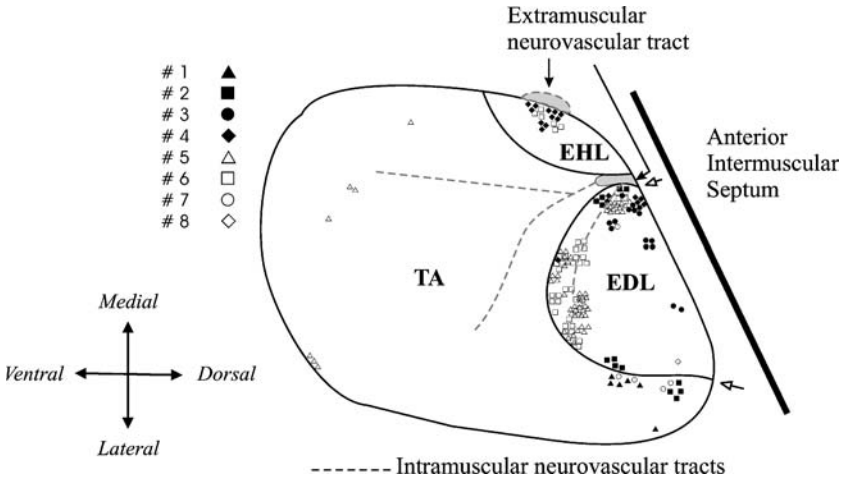

Fig. 4. Location of damaged muscle fibres. A schematic outline in proximal view of the muscles at approximately the middle aspect of the rat anterior crural compartment and the anterior intermuscular septum. The extramuscular and intramuscular neurovascular tracts of several levels within the compartment are projected on this schematic cross-section. In the middle aspect of the compartment, the extramuscular neurovascular tract is located between EHL, TA and EDL muscles. At a more distal level of the compartment, the extramuscular neurovascular tract is located at the medial surface of EHL muscle. Each symbol represents the approximate location of a damaged muscle fibre (i.e. dystrophin, desmin as well as titin negative) with different symbols for each experiment. Damaged fibres were not distributed uniformly throughout the muscle cross-section. Damaged fibres within EDL muscle were located predominantly near the medial and ventral aspect of the interface with TA muscle and the medial interface with the neurovascular tract. Damaged muscle fibres within TA muscle were also located predominantly laterally near the interface with EDL muscle. Anatomical orientation is indicated (cross of arrows).

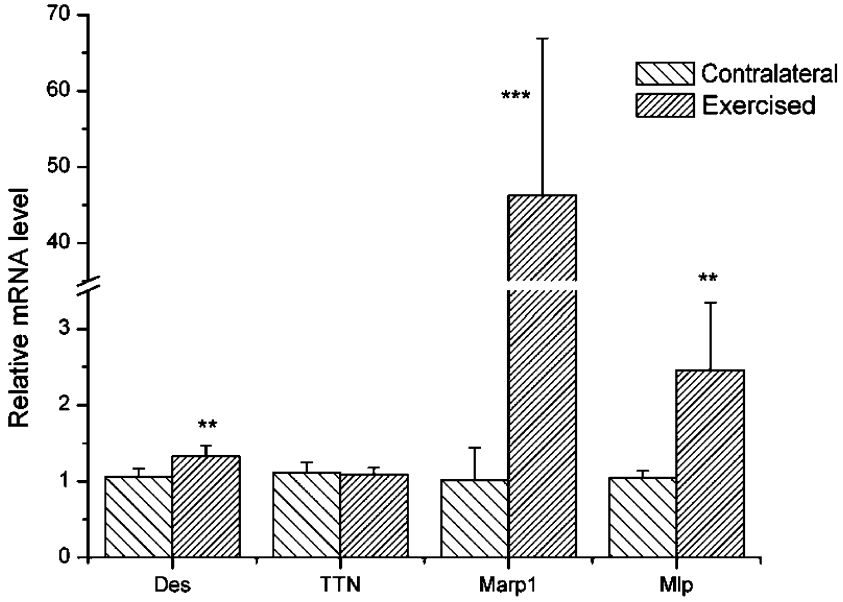

Fig. 5. Quantitative PCR mRNA measurements of desmin (Des), titin (TTN), MARP1, and MLP normalized for GAPDH. Values are shown as mean (SD), $n = 8$. ***$P < 0.001$, **$P < 0.01$ compared with contralateral EDL.

deviated approximately 9 mm from active slack length (Δl_{m+t} EDL III = 0 mm) and force exerted at that length was 0.84 N (SD 0.16).

EDL proximal force (Figure 6b)

Proximal passive EDL force increased exponentially as a function of EDL III length (From 0.02 N, SD 0.01 to 0.08 N, SD 0.07). Proximal active EDL force increased also as a function of EDL III length: from 2.36 N (SD 0.18), at $\Delta l_{m+t} = 0$ mm, to a maximum of 2.53 N (SD 0.23), at $\Delta l_{m+t} = 6.4$ mm. A further increase of EDL III length caused a decrease in proximal EDL force (to 2.43 N, SD 0.33).

These results show that distal lengthening of EDL III caused large changes in force exerted at the distal tendon of EDL III. In contrast, only minor changes were found in force exerted at the proximal EDL tendon. As for mechanical equilibrium, the sum of the forces exerted proximally should equal the sum of the forces exerted distally, these results are explained by force transmission via myofascial pathways between EDL III and its surrounding muscular and/or non-muscular structures.

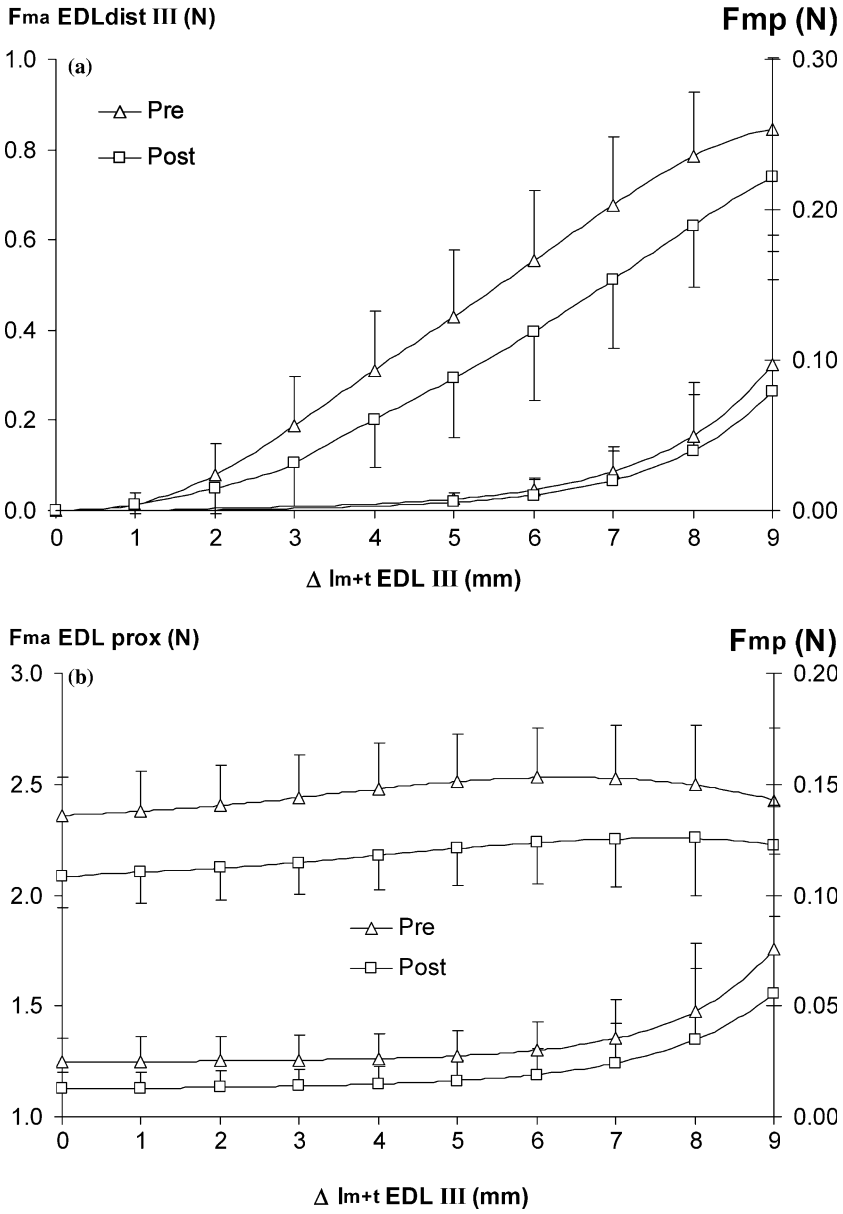

Fig. 6. Effects of prolonged intermittent shortening contractions of EDL III on isometric length–distal force characteristics of EDL III and on proximal EDL force. (a). Length–distal force characteristics EDL III. (b). Active (F_{ma}) and passive (F_{mp}) forces exerted at the proximal EDL tendon plotted as a function of muscle–tendon complex length (Δl_{m+t}) of EDL III. Note that different *y*-axes with different scaling factors are shown for active (left axis) and passive force (right axis). Values are shown as mean (SD), $n=6$.

TA + EHL force (Figure 7)

Passive force exerted by TA + EHL remained negligible. Force exerted at the distal tendons of TA + EHL decreased significantly as a function of lengthening of EDL III distally (i.e. from 5.21 N, SD 0.84 to 5.07 N, SD 0.83) (Figure 4a). These results indicate mechanical interactions between EDL III and TA + EHL, mediated by inter- and/or extramuscular myofascial force transmission.

Effects of prolonged intermittent shortening contractions of EDL III on isometric forces

Distal EDL III force

For passive length–force curves, ANOVA indicated no significant differences between the pre- and post-exercise conditions. In contrast, EDL III length-active force characteristics (Figure 6a) were altered significantly after the exercise of EDL III: at high EDL III lengths ($\Delta l_{m+t}=5$–8 mm), active forces decreased significantly. The slope of the post-exercise length–force curve suggests an optimum length higher than Δl_{m+t} EDL III = 9 mm. As active slack length was not changed, these results indicate that the exercise of EDL III increased the length range between active slack length and optimum length.

Proximal EDL force

Significant effects were found for exercise of EDL III as well as for EDL III muscle–tendon complex length on proximal EDL active and passive forces. For all EDL III lengths tested, passive as well as active force

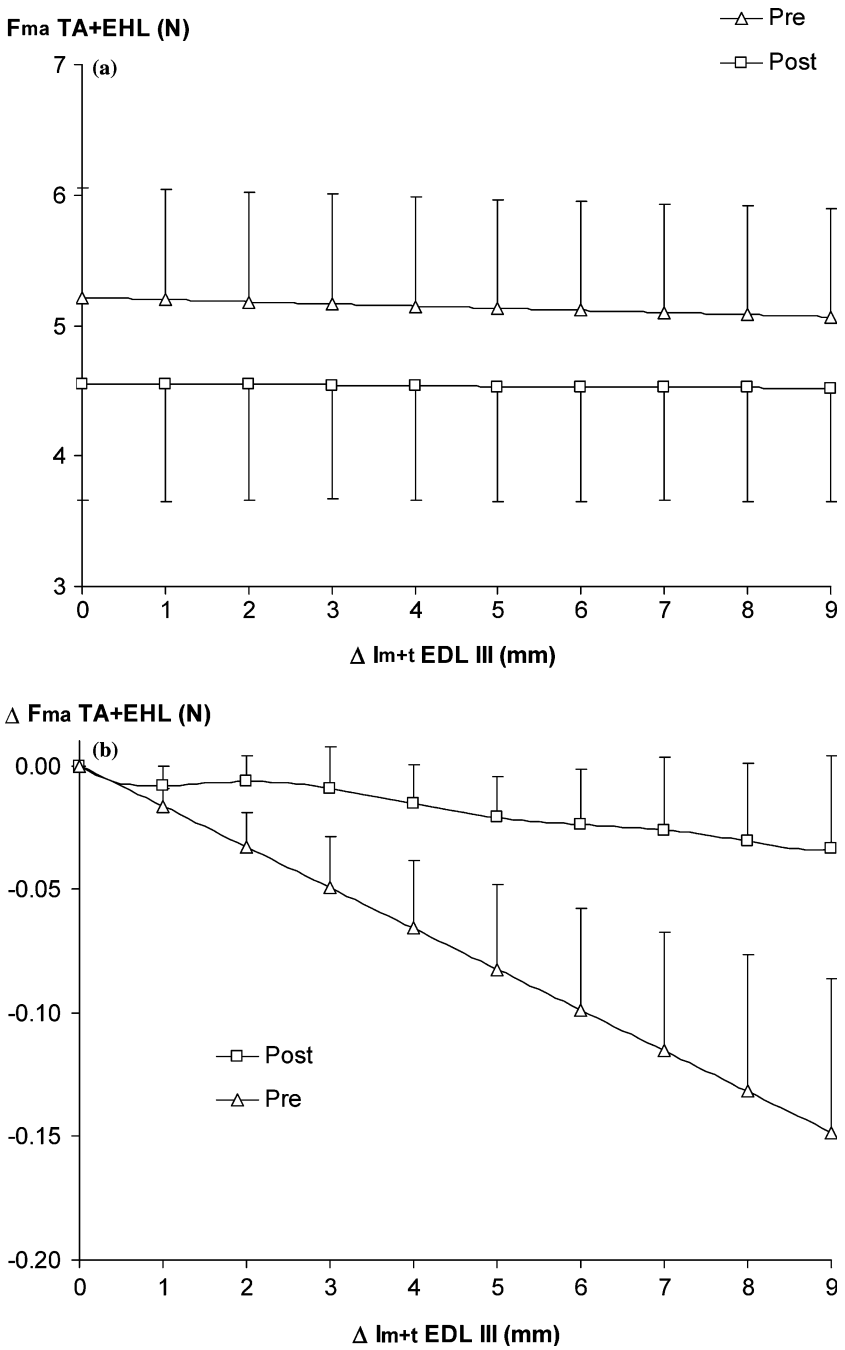

Fig. 7. Effects of prolonged intermittent shortening contractions of EDL III on distally measured active force of the TA + EHL complex, kept at constant muscle–tendon complex length. (a) Absolute values of active forces (F_{ma}) and (b) forces expressed as the deviation (ΔF_{ma}) from the initial value (i.e. measured at active slack length of EDL III, $\Delta l_{m+t} = 0$ mm): F_{ma}, pre = 5.21 N (SD 0.84), F_{ma}, post = 4.55 N (SD 0.89). In both graphs force is plotted as a function of EDL III muscle–tendon complex length (Δl_{m+t}). Values are shown as mean (SD), $n = 6$. The high SDs in A are caused by differences in the initial level of TA + EHL force. Note that the SDs of the change of TA + EHL force (ΔF_{ma}), as shown in (b), are decreased substantially.

of proximal EDL decreased significantly (Figure 6b). No significant interaction between these factors was found, indicating that the pre and post-exercise length–force curves could statistically not be distinguished from being parallel. However, if the effects on maximal EDL force were tested exclusively (paired samples *t*-test), a significant shift to a higher length of EDL III (i.e. from Δl_{m+t} EDL III = 6.4 mm to 7.6 mm) was found.

It should be noted that also post-exercise, changes in proximal EDL force as a function of EDL III muscle–tendon complex length differ substantially from changes of distal EDL III force. Thus, myofascial force transmission between EDL III and adjacent tissues is still present.

TA + EHL force (Figure 7)

For active forces of TA + EHL, ANOVA indicated significant effects of EDL III length as well as of EDL III exercise, and significant interaction between these factors (Figure 7a). For each EDL III length tested,

active TA + EHL force was decreased significantly. In Figure 7b, active force of the TA + EHL is expressed as the deviation from the initial value (F_{ma}, pre = 5.21 N, SD 0.84, F_{ma}, post = 4.55 N, SD 0.89) measured at active slack length of EDL III. As indicated by a significant interaction, the slope of the EDL III length–TA + EHL force curve decreased subsequent to exercise of EDL III. As a consequence, the significant decrease of TA + EHL force after lengthening EDL III by 9 mm was smaller (i.e. 0.03 N, SD 0.04, 0.7%) than the force decrease prior to EDL III exercise (i.e. 0.15 N, SD 0.06, 2.9%).

These results indicate a decrease of the degree of intermuscular interaction between EDL III and TA + EHL. As myofascial force transmission is the proposed mechanism of the interaction, these results may be explained by a decreased stiffness of the myofascial pathways between the muscle belly of EDL III and the muscle bellies of TA and EHL muscles. A decreased stiffness can be the result of (a) altered material properties of structures representing the myofascial pathways and/or (b) a decrease of the number of such structures in parallel. The fibres negative for dystrophin and discontinuous for laminin–2 (Figure 3) near the interface between EDL and TA muscles (Figure 4) indicate that the myofascial route of force transmission is severed for those particular fibres. However, effects on the connective tissues were not studied in the present experiment.

Discussion

The present study showed (a) the presence of damaged muscle fibres only at specific locations within EDL, TA and EHL muscles, (b) the increase in gene expression of Des, MARP1 and MLP, and (c) changes of length–distal force characteristics of EDL III as well as of TA + EHL force after prolonged intermittent shortening activity of EDL III. These results are in agreement with our hypothesis that frequent loading of myofascial pathways may lead to local disturbances or altered mechanical properties of the structures representing those myofascial pathways and, consequently, damaged muscle fibres. The mechanical as well as immunohistochemical changes of TA and EHL muscles indicate that myofascial force transmission is not limited to EDL muscle, but force is also transmitted from EDL III via inter- and/or extramuscular myofascial pathways.

The EDL III exercise caused damage to some muscle fibres, as well as an increase of muscle wet mass of EDL and TA + EHL. Within the exercised legs, the increased muscle wet mass in EDL, as well as in TA + EHL (Table 2) can be explained by swelling of both muscle fibres and the extracellular matrix. After lengthening exercise, the extent of muscle swelling was found to be related to the severity of muscle damage (Komulainen *et al.*, 1994). Immunohistochemical staining of cross-sections of EDL and TA + EHL showed two types of affected fibres: (a) swollen fibres with discontinuous (i.e. fragmented) dystrophin staining, and (b) some of swollen fibres that were fully dystrophin, desmin as well as titin negative and had discontinuous laminin–2 staining (Figure 3). The latter fibres indicate changes in the cytoskeleton (titin and desmin), the subsarcolemmal structures (dystrophin) as well as basement membrane (laminin–2). The loss of staining for dystrophin, desmin and titin are well-documented consequences of lengthening exercise (e.g. Lieber *et al.*, 1996; Komulainen *et al.*, 1998; Lovering and De Deyne, 2004). To the best of our knowledge, this is the first study reporting such protein losses after muscle–tendon complex shortening contractions. In the present study, we also found changes in laminin–2. This may be the result of prolonged and more intensive exercise, as no histopathological changes on laminin–2 were found after a single lengthening contraction (Lovering and De Deyne, 2004) or 30 lengthening contractions (Stauber and Willems, 2002). Laminins are the structural components of the basement membrane and interact with various cell membrane proteins such as dystroglycan (Berthier and Blaineau, 1997). These interactions are important for many basic actions of the cell and disruption of the interaction may lead to muscle fibre damage (Colognato and Yurchenco, 2000; Langenbach and Rando, 2002). Dystrophin is supposed to protect the sarcolemma from high stresses during muscle contraction (Petrof *et al.*, 1993) and, thereby, prevent muscle fibre damage (Straub *et al.*, 1997). After lengthening exercise, the loss of dystrophin staining occurred before the disruption of the contractile apparatus (Komulainen *et al.*, 1998). Therefore, muscle fibre damage may be a result of disrupted dystrophin structure.

The extent of histopathological changes 3 h after the cessation of EDL III exercise was minor (Table 2), but is typical in the time course of muscle fibre injury following muscle lengthening contractions (Lieber *et al.* 1996; Komulainen *et al.*, 1998). Those studies also reported that 2 days after lengthening exercise, the number of dystrophin and desmin negative fibres had increased substantially and that the inflammation was in a progress. If it is assumed that muscle damage observed in the present study would develop in a similar way, more severe structural changes in muscle architecture will be found later after exercise.

The results of this study showed that the damaged muscle fibres were not distributed uniformly throughout the muscle cross-sections. Damage within the medial-ventral part of EDL muscle, within EHL muscle and within the medial-ventral part of TA muscle was found near intra- and extramuscular locations of the neurovascular tracts (Figure 4). These tracts are thick sheets of connective tissue, embedding major nerves and blood vessels. The neurovascular tracts are continuous with the endomysial-perimysial stroma (Huijing *et al.*, 2003). It has been shown that the extramuscular neurovascular tract can transmit force out of muscle

(Maas *et al*., 2003). A main effect of the connective tissue of the tract is the protection of the nerves and blood vessels from excessive strain: The collagen fibres act as fibre reinforcement of a much less stiff matrix and bear most of the load. Correspondingly, this connective tissue is rather stiff. As of parallel pathways, the pathway with the stiffest properties will transmit the greatest fraction of force, neurovascular tracts are prominent candidates for force transmission. Damaged muscle fibres near extra- and intramuscular neurovascular tracts suggest that high forces were borne by these tracts during the exercise of EDL III. Therefore, a detailed anatomical description of the 3D position of these tracts within the compartment and its muscles is essential for the understanding of *in vivo* muscular force transmission.

In contrast to the studies reporting on effects of lengthening exercise, in the present study, EDL III muscle–tendon complex was lengthened only while in the passive state, which was followed by active shortening. The muscle–tendon complex length of the other heads of EDL muscle (i.e. II, IV and V) and the TA + EHL complex was kept constant. Previous studies reported no immunohistochemical or histological signs of muscle damage at 0 h through 15 days after shortening or isometric exercise of TA and/or whole EDL muscle (McCully and Faulkner, 1985; Lieber *et al*., 1991; Hesselink *et al*., 1996, 1998; Komulainen *et al*., 2000). Note that several conditions of the studies above are different from the present experimental conditions: (a) the number of contractions was lower (between 240 and 1800 compared to 10,800 in the present study), (b) the lengths of several muscles were altered simultaneously, as length changes of the muscles were obtained by joint movements (Hesselink *et al*., 1996, 1998; Komulainen *et al*., 2000), (c) the fully recruited muscle was activated submaximally (Lieber *et al*., 1991), (d) the time between the start of stimulation and the start of shortening, the shortening velocity, and the magnitude of shortening were different, and (e) other animals, i.e. mouse EDL muscle (McCully and Faulkner, 1985) and rabbit TA muscle (Lieber *et al*., 1991), were studied. It should be noted that in the present work only one control group, i.e. the unexercised contralateral muscles, was used. Therefore, it cannot be excluded that 3 h of isometric or lengthening contractions would have yielded similar results. However, preliminary data indicate that muscles exposed exclusively to length–force measurements ($n = 1$) or to prolonged (3 h) passive sinusoidal length changes of EDL III ($n = 1$) do not show any indices of muscle damage.

Changes in gene expression of studied proteins also show clear effects of prolonged exercise as such used in the present study. Desmin and titin are sarcomeric non-contractile proteins. Desmin is located within Z-lines as well as between Z-lines of adjacent myofibrils and may play an important role in linking the sarcomeres to subsarcolemmal actin structures and thus in myofascial force transmission. Titin forms a spring from Z-line to A-band and is the only molecule that extends over half a sarcomere. In this study the transcription of desmin was shown to be elevated already 3 h after the shortening exercise. Peters *et al*. (2003) observed significant increases not earlier than 12 h after lengthening exercise, having its peak value 48 h post-exercise. This suggests that sampling of our muscles at a later time after exercise may have shown a more prominent increase in desmin mRNA content. Exercise as such had no effect on the expression of Ttn at the studied time point, but the immunohistochemical staining of titin was lost. There are only a few studies of titin in context of muscle fibre damage (Lieber *et al*., 1996; Yu *et al*., 2003). Abnormal titin staining was observed previously already after 30 min following 30 min of lengthening contractions (Lieber *et al*., 1996) and lack of staining 2–3 days after the exercise (Yu *et al*., 2003). Reappearance of titin staining occurred after several (7–8) days (Yu *et al*., 2003), which indicates a delay in the upregulation of Ttn after muscle fibre damage. Preliminary results also indicate such a delay for titin after downhill running (Lehti *et al*., unpublished observations). Therefore, it is concluded that the observation time point of the present study was too early to show an increase in titin transcription.

In contrast, transcription of two titin associated proteins, MARP1 and MLP, was significantly increased in the present study, as well as after lengthening exercise in a previous study (Barash *et al*., 2004). MARP1 interacts with titin in I-bands (Bang *et al*., 2001; Miller *et al*., 2003) and MLP interacts with titin indirectly through T-cap (also known as teletonin) (Knoll *et al*., 2002). Interaction of T-cap and titin at the Z-line is required for the structural integrity of sarcomeres (Gregorio *et al*., 1998). MARP1 and MLP together with titin have been proposed to be involved in a stretch sensing action in the muscle (reviewed in Miller *et al*., 2004). Miller *et al*. (2003) showed that immunostaining of MARP1 (also known as cardiac ankyrin repeat protein, CARP) is more intense in cardiac myocytes after passive stretch (10–12%). They assumed that MARPs may have a key role in controlling muscle gene expression as they are regulated by stretch and are located both in the nucleus and cytoplasm. In addition to Z-line proteins, MLP has a capacity to interact with costamere proteins (Flick and Konieczny, 2000). Through transcription factor MyoD, MLP may also have a function promoting myogenesis in the nucleus (Geier *et al*., 2003). For these interactions MLP is a probable stress sensor and gene expression regulator in the muscle. Our findings of the increase in gene expression of MARP1 and MLP at the early time point support regulative role of these proteins in the course of contraction-induced muscle adaptation.

A possible mechanism responsible for the immunohistochemical identified damaged muscle fibres as well as for the increased gene expression of sarcomeric

proteins after EDL III exercise, as found in the present experiment, may be local lengthening of active sarcomeres. It is proposed here that active shortening of the EDL III muscle–tendon complex causes lengthening contractions locally within muscle fibres of adjacent EDL heads as well as TA and EHL. Finite element modelling of distally shortening whole EDL muscle indicated an increase of length of sarcomeres located within muscle fibres near the distal aponeurosis as well as a decrease of length of sarcomeres located within muscle fibres near the proximal aponeurosis within the restrained synergists (Yucesoy *et al*., 2003). Note that such distributions of lengths of sarcomeres within muscle fibres are possible due to the presence of myofascial force transmission. If the length of a muscle is altered dynamically, as in the present experiment for EDL III, these finite element modelling results suggest that dynamic distal shortening of EDL III may have been accompanied by active lengthening of sarcomeres near the distal aponeuroses of the other heads of EDL muscle as well as of TA and EHL muscles. It is concluded that shortening contractions of a muscle–tendon complex may involve lengthening contractions at the level of the sarcomere within muscle fibres of adjacent muscle bellies. It is thus important to describe local effects of changes in relative position of muscles when considering experimental protocols.

After the EDL III exercise, the length range between active slack length and optimum length was increased due to a shift of optimum length of EDL III to higher lengths (Figure 6a). In addition, maximal EDL active force exerted at the proximal tendon shifted also to a higher length of EDL III. Factors that have been shown to affect this length range are: (a) Muscular fatigue (Blix, 1894; Gauthier *et al*., 1993; Ralston *et al*., 1947). However, in the present study, the muscles were allowed to recover until isometric muscle force remained constant and the shape of the time–force trace resembled that of an isometric tetanic contraction of a muscle in the unfatigued state. (b) The distribution of lengths of sarcomeres arranged in series within muscle fibres (Huxley and Peachey, 1961; Granzier and Pollack, 1990; Pollack *et al*., 1993), and (c) the distribution of fibre mean sarcomere length (Ettema and Huijing, 1994; Willems and Huijing, 1994). Finite element modelling has shown that such distributions are affected as a result of more compliant connections between muscle fibre and extracellular matrix (Yucesoy *et al*., 2002). As dystrophin and laminin−2 are links in the myofascial chain, this compliance will be increased for the fibres with discontinuous dystrophin and laminin−2 staining or dystrophin negative fibres (Figure 3). In addition, inter- and extramuscular connective tissues have been shown to affect the serial distribution of lengths of sarcomeres in series as well as the distribution of fibre mean sarcomere length (parallel distribution) (Maas *et al*., 2003; Yucesoy *et al*., 2003). The decreased intermuscular interaction between EDL III and TA + EHL post-exercise (Figure 7) indicates altered mechanical properties of the connections between these muscles. (d) The elastic compliance in series with the sarcomeres (Lieber *et al*., 1992; Komulainen and Vihko, 1994; Kawakami and Lieber, 2000). For EDL III this is represented by its aponeuroses and tendons, elastic structures within its muscle belly (e.g. endomysium, epimysium, *trans*-sarcolemmal linkages, titin) as well as elastic structures that link the muscle belly of EDL III to adjacent tissues (i.e. intra-, inter-, and extramuscular connective tissues). The following results of the present work indicate an increase of the series elastic compliance of EDL III: (1) dystrophin, desmin and titin negative muscle fibres as well as fibres with discontinuous laminin−2, (2) the decreased intermuscular interaction between EDL III and TA + EHL.

In conclusion, prolonged intermittent shortening contractions of a single muscle head of multi-tendoned muscle causes damage to muscle fibres within that head as well as to muscle fibres within the other heads and adjacent muscles. Furthermore, such exercise alters force transmission from the exercised muscle head, as well as its mechanical interaction with surrounding tissues. These results can be explained by effects of myofascial force transmission.

Acknowledgements

Prof. Peter Yurchenco (Department of Pathology and Laboratory Medicine, UMDNJ-Robert Wood Johnson Medical School, Piscataway, NJ 08554–56) generously provided rabbit polyclonal laminin−2 antibody. Grants: This study was supported by LIKES-foundation and the Ministry of Education, Finland.

References

Balice-Gordon RJ and Thompson WJ (1988) The organization and development of compartmentalized innervation in rat extensor digitorum longus muscle. *J Physiol* **398:** 211–231.

Bang ML, Mudry RE, McElhinny AS, Trombitas K, Geach AJ, Yamasaki R, Sorimachi H, Granzier H, Gregorio CC and Labeit S (2001) Myopalladin, a novel 145-kilodalton sarcomeric protein with multiple roles in Z-disc and I-band protein assemblies. *J Cell Biol* **153:** 413–427.

Barash IA, Mathew L, Ryan AF, Chen J and Lieber RL (2004) Rapid muscle-specific gene expression changes after a single bout of eccentric contractions in the mouse. *Am J Physiol Cell Physiology* **286:** C355–C364.

Berthier C and Blaineau S (1997) Supramolecular organization of the subsarcolemmal cytoskeleton of adult skeletal muscle fibers. A review. *Biol Cell* **89:** 413–434.

Blix M (1894) Die länge und spannung des muskels: vierte abhandlung. *Skandinavische Archiv für Physiologie* **V:** 173–206.

Boriek AM, Zhu D, Zeller M and Rodarte JR (2001) Inferences on force transmission from muscle fiber architecture of the canine diaphragm. *Am J Physiol Regul Integr Comp Physiol* **280:** R156–R165.

Colognato H and Yurchenco PD (2000) Form and function: the laminin family of heterotrimers. *Develop Dyn* **218:** 213–234.

Ettema GJC and Huijing PA (1994) Effects of distribution of muscle fiber length on active length–force characteristics of rat gastrocnemius medialis. *Anat Rec* **239:** 414–420.

Field KJ and Lang CM (1988) Hazards of urethane (ethyl carbamate): a review of the literature. *Lab Animals* **22:** 255–262.

Flick MJ and Konieczny SF (2000) The muscle regulatory and structural protein MLP is a cytoskeletal binding partner of betaI-spectrin. *J Cell Sci* **113:** 1553–1564.

Friden J, Lieber RL and Thornell LE (1991) Subtle indications of muscle damage following eccentric contractions. *Acta Physiol Scand* **142:** 523–524.

Gauthier AP, Faltus RE, Macklem PT and Bellemare F (1993) Effects of fatigue on the length–tetanic force relationship of the rat diaphragm. *J Appl Physiol* **74:** 326–332.

Geier C, Perrot A, Ozcelik C, Binner P, Counsell D, Hoffmann K, Pilz B, Martiniak Y, Gehmlich K, van der Ven PF, Furst DO, Vornwald A, von Hodenberg E, Nurnberg P, Scheffold T, Dietz R and Osterziel KJ (2003) Mutations in the human muscle LIM protein gene in families with hypertrophic cardiomyopathy. *Circulation* **107:** 1390–1395.

Granzier HL and Pollack GH (1990) The descending limb of the force–sarcomere length relation of the frog revisited. *J Physiol* **421:** 595–615.

Gregorio CC, Trombitas K, Centner T, Kolmerer B, Stier G, Kunke K, Suzuki K, Obermayr F, Herrmann B, Granzier H, Sorimachi H and Labeit S (1998) The NH_2 terminus of titin spans the Z-disc: its interaction with a novel 19-kD ligand (T-cap) is required for sarcomeric integrity. *J Cell Biol* **143:** 1013–1027.

Hesselink MK, Kuipers H, Geurten P and Van Straaten H (1996) Structural muscle damage and muscle strength after incremental number of isometric and forced lengthening contractions. *J Muscle Res Cell Motil* **17:** 335–341.

Hesselink MK, Kuipers H, Keizer HA, Drost MR and van der Vusse GJ (1998) Acute and sustained effects of isometric and lengthening muscle contractions on high-energy phosphates and glycogen metabolism in rat tibialis anterior muscle. *J Muscle Res Cell Motil* **19:** 373–380.

Huijing PA, Baan GC and Rebel GT (1998) Non-myotendinous force transmission in rat extensor digitorum longus muscle. *J Exp Biol* **201:** 683–691.

Huijing PA (1999) Muscle as a collagen fiber reinforced composite: a review of force transmission in muscle and whole limb. *J Biomech* **32:** 329–345.

Huijing PA, Maas H and Baan GC (2003) Compartmental fasciotomy and isolating a muscle from neighboring muscles interfere with myofascial force transmission within the rat anterior crural compartment. *J Morphol* **256:** 306–321.

Huxley AF and Peachey LD (1961) The maximum length for contraction in vertebrate striated muscle. *J Physiol* **156:** 150–165.

Kawakami Y and Lieber RL (2000) Interaction between series compliance and sarcomere kinetics determines internal sarcomere shortening during fixed-end contraction. *J Biomech* **33:** 1249–1255.

Kjaer M (2004) Role of extracellular matrix in adaptation of tendon and skeletal muscle to mechanical loading. *Physiol Rev* **84:** 649–698.

Knoll R, Hoshijima M, Hoffman HM, Person V, Lorenzen-Schmidt I, Bang ML, Hayashi T, Shiga N, Yasukawa H, Schaper W, McKenna W, Yokoyama M, Schork NJ, Omens JH, McCulloch AD, Kimura A, Gregorio CC, Poller W, Schaper J, Schultheiss HP and Chien KR (2002) The cardiac mechanical stretch sensor machinery involves a Z disc complex that is defective in a subset of human dilated cardiomyopathy. *Cell* **111:** 943–955.

Knoll R, Hoshijima M and Chien K (2003) Cardiac mechanotransduction and implications for heart disease. *J Mol Med* **81:** 750–756.

Komulainen J, Kytola J and Vihko V (1994) Running-induced muscle injury and myocellular enzyme release in rats. *J Appl Physiol* **77:** 2299–2304.

Komulainen J and Vihko V (1994) Exercise-induced necrotic muscle damage and enzyme release in the four days following prolonged submaximal running in rats. *Pflügers Archiv* **428:** 346–351.

Komulainen J, Takala TE, Kuipers H and Hesselink MK (1998) The disruption of myofibre structures in rat skeletal muscle after forced lengthening contractions. *Pflügers Archiv* **436:** 735–741.

Komulainen J, Kalliokoski R, Koskinen SO, Drost MR, Kuipers H and Hesselink MK (2000) Controlled lengthening or shortening contraction-induced damage is followed by fiber hypertrophy in rat skeletal muscle. *Int J Sports Med* **21:** 107–112.

Langenbach KJ and Rando TA (2002) Inhibition of dystroglycan binding to laminin disrupts the PI3K/AKT pathway and survival signaling in muscle cells. *Muscle Nerve* **26:** 644–653.

Lazarides E (1980) Intermediate filaments as mechanical integrators of cellular space. *Nature* **283:** 249–256.

Lieber RL, Woodburn TM and Fridén J (1991) Muscle damage induced by eccentric contractions of 25% strain. *J Appl Physiol* **70:** 2498–2507.

Lieber RL, Brown CG and Trestik CL (1992) Model of muscle–tendon interaction during frog semitendinosis fixed-end contractions. *J Biomech* **25:** 421–428.

Lieber RL, Thornell LE and Friden J (1996) Muscle cytoskeletal disruption occurs within the first 15 min of cyclic eccentric contraction. *J Appl Physiol* **80:** 278–284.

Lovering RM and De Deyne PG (2004) Contractile function, sarcolemma integrity, and the loss of dystrophin after skeletal muscle eccentric contraction-induced injury. *Am J Physiol Cell Physiol* **286:** C230–C238.

Maas H, Baan GC, Huijing PA, Yucesoy CA, Koopman BH and Grootenboer HJ (2003) The relative position of EDL muscle affects the length of sarcomeres within muscle fibers: experimental results and finite-element modeling. *J Biomech Eng* **125:** 745–753.

Maas H, Jaspers RT, Baan GC and Huijing PA (2003) Myofascial force transmission between a single muscle head and adjacent tissues: length effects of head III of rat EDL. *J Appl Physiol* **95:** 2004–2013.

Mass H and Huijing PA (2005) Myofascial force transmission in dynamic muscle conditions: effects of dynamic shortening of a single head of multi-tendoned rat extensor digitorum longus muscle. *Eur J Appl Physiol* **94:** 584–592.

McCully KK and Faulkner JA (1985) Injury to skeletal muscle fibers of mice following lengthening contractions. *J Appl Physiol* **59:** 119–126.

Miller MK, Bang ML, Witt CC, Labeit D, Trombitas C, Watanabe K, Granzier H, McElhinny AS, Gregorio CC and Labeit S (2003) The muscle ankyrin repeat proteins: CARP, ankrd2/Arpp and DARP as a family of titin filament-based stress response molecules. *J Mol Biol* **333:** 951–964.

Miller MK, Granzier H, Ehler E and Gregorio CC (2004) The sensitive giant: the role of titin-based stretch sensing complexes in the heart. *Trends Cell Biol* **14:** 119–126.

Monti RJ, Roy RR, Hodgson JA and Edgerton VR (1999) Transmission of forces within mammalian skeletal muscles. *J Biomech* **32:** 371–380.

Peters D, Barash IA, Burdi M, Yuan PS, Mathew L, Friden J and Lieber RL (2003) Asynchronous functional, cellular and transcriptional changes after a bout of eccentric exercise in the rat. *J Physiol* **553:** 947–957.

Petrof BJ, Shrager JB, Stedman HH, Kelly AM and Sweeney HL (1993) Dystrophin protects the sarcolemma from stresses developed during muscle contraction. *Proc Natl Acad Sci USA* **90:** 3710–3714.

Pollack GH, Horowitz A, Wussling M and Trombitas K (1993) Shortening-induced tension enhancement: implication for length–tension relations. *Adv Exp Med Biol* **332:** 679–688 discussion 688–690.

Price MG (1987) Skelemins: cytoskeletal proteins located at the periphery of M-discs in mammalian striated muscle. *J Cell Biol* **104:** 1325–1336.

Price MG and Gomer RH (1993) Skelemin, a cytoskeletal M-disc periphery protein, contains motifs of adhesion/recognition and intermediate filament proteins. *J Biol Chem* **268:** 21800–21810.

Purslow PP (2002) The structure and functional significance of variations in the connective tissue within muscle. *Comp Biochem Physiol A Mol Integr Physiol* **133:** 947–966.

Ralston HJ, Inman VT, Strait LA and Shaffrath MD (1947) Mechanics of human isolated voluntary muscle. *Am J Physiol* **151:** 612–620.

Spofford CM and Chilian WM (2003) Mechanotransduction via the elastin-laminin receptor (ELR) in resistance arteries. *J Biomech* **36:** 645–652.

Stauber WT and Willems ME (2002) Prevention of histopathologic changes from 30 repeated stretches of active rat skeletal muscles by long inter-stretch rest times. *Eur J Appl Physiol* **88:** 94–99.

Straub V, Rafael JA, Chamberlain JS and Campbell KP (1997) Animal models for muscular dystrophy show different patterns of sarcolemmal disruption. *J Cell Biol* **139:** 375–385.

Street SF and Ramsey RW (1965) Sarcolemma transmitter of active tension in frog skeletal muscle. *Science* **149:** 1379–1380.

Street SF (1983) Lateral transmission of tension in frog myofibres: a myofibrillar network and transverse cytoskeletal connections are possible transmitters. *J Cell Physiol* **114:** 346–364.

Tidball JG (1991) Force transmission across muscle cell membranes. *J Biomech* **24:** 43–52.

Trotter JA (1993) Functional morphology of force transmission in skeletal muscle. A brief review. *Acta Anatomica* **146:** 205–222.

Willems MET and Huijing PA (1994) Heterogeneity of mean sarcomere length in different fibres: effects on length range of active force production in rat muscle. *Eur J Appl Physiol* **68:** 489–496.

Woittiez RD, Brand C, de Haan A, Hollander AP, Huijing PA, van der Tak R and Rijnsburger WH (1987) A multipurpose muscle ergometer. *J Biomechs* **20:** 215–218.

Yu JG, Furst DO and Thornell LE (2003) The mode of myofibril remodelling in human skeletal muscle affected by DOMS induced by eccentric contractions. *Histochem Cell Biol* **119:** 383–393.

Yucesoy CA, Koopman BHFJM, Huijing PA and Grootenboer HJ (2002) Three-dimensional finite element modeling of skeletal muscle using a two-domain approach: linked fiber-matrix mesh model. *J Biomech* **35:** 1253–1262.

Yucesoy CA, Koopman BH, Baan GC, Grootenboer HJ and Huijing PA (2003) Effects of inter- and extramuscular myofascial force transmission on adjacent synergistic muscles: assessment by experiments and finite-element modeling. *J Biomech* **36:** 1797–1811.